Intensity interference in Bragg scattering by acoustic waves with thermal statistics

M. V. Chekhova, S. P. Kulik, A. N. Penin, and P. A. Prudkovskii
Department of Quantum Radiophysics, Moscow State University, 119899 Moscow, Russia

(Received 5 February 1996; revised manuscript received 8 August 1996)

Angular distributions of the intensity and the fourth-order correlation function are studied for light scattered by acoustic waves with thermal statistics. In the case when the beam diameter exceeds the coherence length of the acoustic wave, the fourth-order correlation function is found to contain an interference structure, whereas the intensity angular distribution has a one-peak shape. [S1050-2947(96)50911-X]

PACS number(s): 42.50.Ar, 42.25.Hz

Does the intensity correlation function (the fourth-order correlation function, in Glauber's notation) provide any information that is not contained in the intensity distribution? For coherent light and for light with thermal statistics, the answer is at first sight trivial: higher-order intensity moments can be expressed via the average intensity. On the other hand, the well-known experiment by Brown and Twiss [1] demonstrated that the measurement of the intensity correlation function has some advantages over the measurement of the field correlation function. In particular, it was successfully used for determining the angular diameters of stars [2].

There is no contradiction in these two statements. The fourth-order correlation function differs essentially from the second-order one, whenever the light under study contains a superposition of independent fields. As a simple example, one can consider the interference from two monochromatic sources with thermal statistics: if the sources are independent, they form no second-order interference pattern, but the fourth-order correlation function contains interference fringes, which can be used for measuring the angular distance between the sources [3].

In the present paper we show how the measurement of the intensity correlation function of light scattered by acoustic waves can provide information that is not contained in the intensity distribution. The experimental setup is shown in Fig. 1. A single-model He-Ne laser beam, whose aperture l can be varied by means of the diaphragm $D0$ within the range 0.8–3 mm, is directed into a block of fused silica (FS). In the silica the beam is scattered by an acoustic wave propagating normally to the beam. The acoustic wave has quasithermal statistics, for it is excited in the following way. A photomultiplier tube (PMT0) operating in a photon counting regime is illuminated by the radiation of a stabilized light-emitting diode (LD), and its amplified pulses form a continuous spectral distribution in the frequency range from 10 to 100 MHz. This ''white noise'' is sent to a narrow-band active filter (AF), which amplifies the signal within the band of $\delta f=2.5$ MHz with central frequency $f=\Omega/2\pi=50$ MHz. According to the principles of statistical radiophysics, such a procedure gives a random signal with Gaussian (thermal) statistics. The spectrum of the electric signal is analyzed by means of a spectrum analyzer (SA). This signal is fed to a piezoelectric element (PE), which is used to generate the acoustic wave in the silica. Thus, we obtain a quasithermal acoustic wave with coherence length 1.5 mm. Light scattered by this quasithermal wave must also possess thermal statistics. This fact, perhaps obvious enough, is to be discussed in detail in Ref. [4]; for its theoretical proof, see Ref. [5].

Light scattered at the Bragg angle is analyzed by means of the Brown-Twiss interferometer. It is split by a beam splitter (BS) and the two beams are fed to a pair of photon counting photomultipliers (PMT1 and PMT2). The output pulses of the PMT's are sent to a digital correlator CORR that provides the coincidence counting rate R_c and the counting rates of both detectors R_1 and R_2. An IBM personal computer calculates the normalized second intensity moment, the bunching parameter $g^{(2)}=\langle I^2\rangle/\langle I\rangle^2$, which is related to R_c as $g^{(2)}=R_c/R_1R_2\tau$, time parameter τ being determined by the resolution of the correlator. The distance between the sample and each of the detectors $L=5$ m; that is, the scattering is observed in the far field zone. A 0.4-mm diaphragm (D1) at the input of PMT1 selects radiation scattered at the Bragg angle. At the input of the other PMT the angle of scattering is scanned by means of an adjustable 0.4-mm diaphragm $D2$ connected by fiber F with the PMT. The diaphragm can be displaced within the vicinity of 15 mm, this corresponding to the scattering angle variation by 0.2°.

The experimental results are represented by R_c/R_1R_2 and R_2 plotted against the coordinate of $D2$. The first value is equal to $g^{(2)}$ multiplied by the effective coincidence resolution τ, which was equal to 7.5 ns. We obtained a set of such dependences for the following diameters of the pump beam:

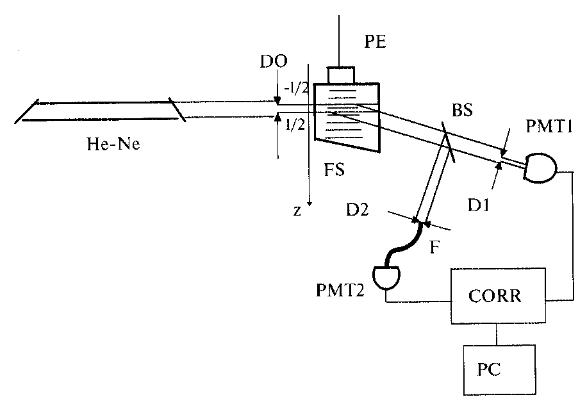

FIG. 1. The experimental setup. LD, light-emitting diode; PMT0, PMT1, PMT2, photomultiplier tubes; AF, active filter; SA, spectrum analyzer; PE, piezoelectric element; FS, fused silica; $D0$, diaphragm with variable diameter; BS, beam splitter; $D1$ and $D2$, pinholes; F, fiber; CORR, correlation circuit; PC, computer.

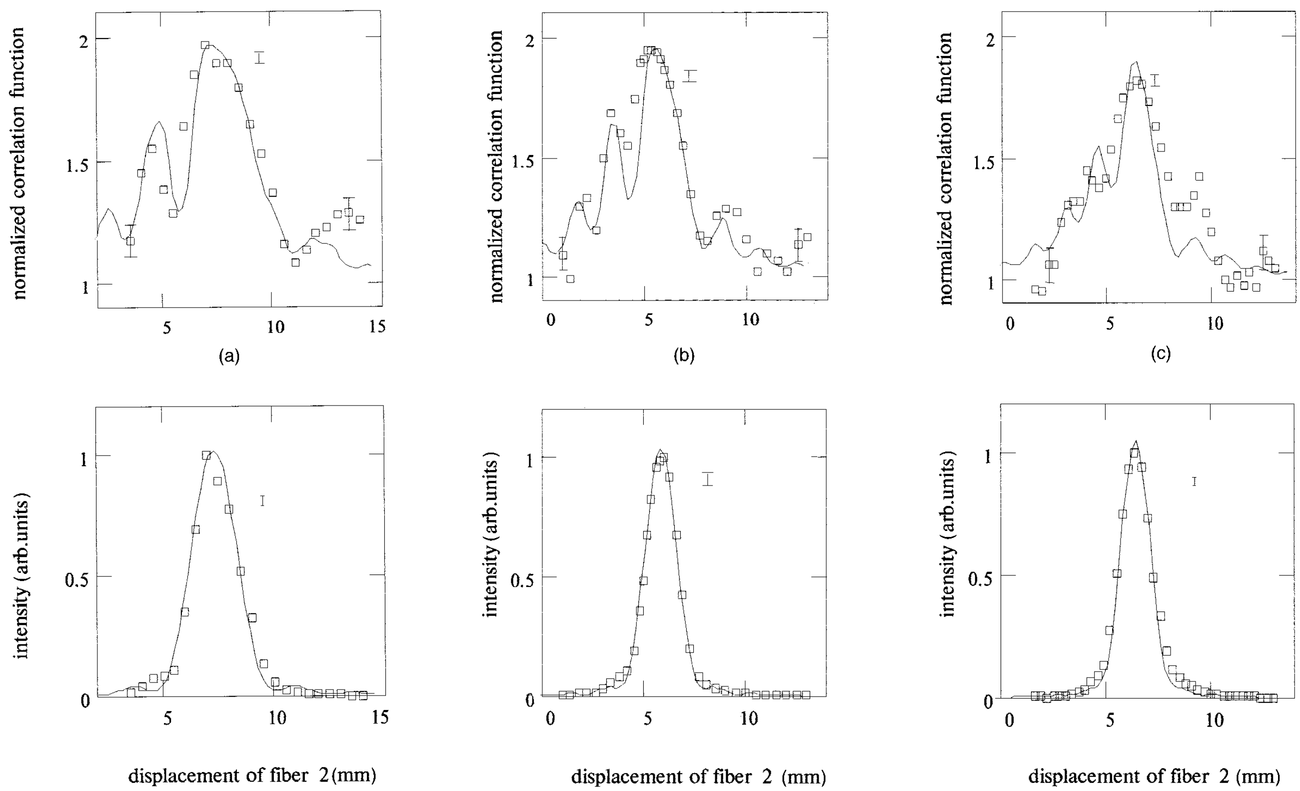

FIG. 2. Upper plots: angular distributions of the normalized correlation function; lower plots: normalized intensity distributions for the diffracted beam. Experimental points are shown as squares; theoretical dependences are plotted as solid curves. Displacement of fiber 2 in the far field zone corresponds to the difference between the angle of observation and the Bragg angle. Diameters of the diaphragm $D0$ are 1.5 mm (a), 2 mm (b), and 2.5 mm (c).

0.8, 1.5, 2, 2.5, and 3 mm. For the beam of 0.8 mm width the normalized correlation function has rather weak dependence on the angle of scattering, and the bunching parameter is near 2 in the whole area where the signal is observed. For larger $D0$ apertures the normalized correlation function has oscillating angular dependence. At the same time, corresponding angular intensity (R_2) distributions contain no or almost no oscillations. Three typical plots relating to the beam diameters 1.5, 2, and 2.5 mm are shown in Fig. 2 (separate points). The oscillations become more frequent with the increase of the aperture of $D0$. For the beam diameter 1.5 mm, the oscillations become less frequent.

In order to describe the oscillating behavior of the correlation function, we calculate the total field scattered at a given direction. The scattering volume is formed by the intersection of the pump beam with the area where the acoustic wave is propagating. Due to the geometry of the experiment, the scattering volume has cylindrical shape, its axis coinciding with the pump direction, and the diameter is determined by the size of $D0$ (see Fig. 1). The longitudinal size of the cylinder is much larger, so the angular spectrum of scattering can be described in terms of transverse wave-vector mismatch $\Delta \equiv k_s^z + k_a$, where k_s^z is the wave-vector transverse component for the scattered wave. (The axis z is transverse for the pump propagation; it coincides with the direction of the acoustic wave.) The wave vector of the acoustic wave is denoted by k_a. The acoustic signal is determined by the voltage applied to the piezoelectric element. The voltage depends on time as a random Gaussian signal and can be written in the form

$$U(t) = U_0(t)\exp[i\phi(t)]\exp[i\Omega t],$$

$U_0(t)$ and $\phi(t)$ representing the random amplitude and random phase of the signal, respectively. Hence, the acoustic wave propagating along z is also characterized by the random amplitude $Q_0(z)$ and random phase $\phi(z)$,

$$Q(z) = Q_0(z)\exp[i\phi(z)]\exp(ik_a z - i\Omega t). \qquad (1)$$

Its coherence length Λ is determined by δf and equals 1.5 mm.

The scattered light is then described by the analytic signal [6],

$$E_s(\Delta) \propto \int_{-l/2}^{l/2} Q_0(z)\exp\{[i\phi(z) + i\Delta z]dz\}. \qquad (2)$$

The integration is done over the aperture of the diaphragm $D0$. For simplicity we consider here the case of a one-dimensional diaphragm, although in the experiment the diaphragm is round.

The intensity measured by each PMT can be written as

$$I_i=\langle|E_s^{(i)}|^2\rangle\propto\int\int_{-l/2}^{l/2}\langle Q_0(z)Q_0(z')\exp\{i[\phi(z)-\phi(z')]+i\Delta(z-z')\}\rangle dz\,dz', \quad (3)$$

the index $i=1,2$ relating to the PMT. The intensity correlator $g^{(2)}=\langle I_1I_2\rangle/\langle I_1\rangle\langle I_2\rangle$ can be calculated quite similarly.

We use a Gaussian correlation function for the distribution of the quasithermal acoustic wave,

$$B(z-z')\equiv\langle Q_0(z)Q_0(z')\exp\{i[\phi(z)-\phi(z')]\}\rangle=\frac{1}{\Lambda}\sqrt{\frac{2}{\pi}}\exp\left[\frac{-(z-z')^2}{2\Lambda^2}\right]. \quad (4)$$

After simple calculations, we obtain the following expressions for the intensity and the correlation function:

$$I_i=2\int_0^l yB(y)(l-y)\cos(\Delta_i y)dy, \quad g^{(2)}=1+\frac{|J_{12}|^2}{I_1I_2}, \quad (5)$$

where

$$J_{12}=\frac{2}{\Delta}\int_0^l B(y)[\sin(\Delta_1 y+\Delta l/2)-\sin(\Delta_2 y-\Delta l/2)]dy,$$

$$\Delta\equiv\Delta_1-\Delta_2.$$

Distributions of I_i and $g^{(2)}$ have been calculated numerically as functions of the dimensionless phase mismatch $x=\Delta\Lambda$. Note that the phase mismatch Δ_i is related to the displacement of the corresponding PMT, x_i, as $\Delta_i=2\pi x_i/\lambda_s L$, where λ_s is the scattered light wavelength (633 nm).

The calculated intensity and correlation function distributions depend on the ratio l/Λ. When the beamwidth is smaller than the coherence length of the acoustic wave, then light scattered at different points of the scattering volume interferes and forms an oscillating intensity distribution close to sin$c(\Delta l)$. At the same time, the acoustic wave amplitude fluctuates in this case synchronously in the scattering volume, which is smaller than the coherence volume. Then the normalized correlation function should be equal to ''2'' in a wide angular range, as for a pointlike thermal source. This explains why for small diaphragm apertures (0.8 mm) we observed a broad distribution of the normalized correlation function, its maximal value being equal to 2. As the beam diameter becomes larger than the coherence length of the acoustic wave, the intensity line shape loses its interference character and acquires the form of a single peak. However, according to our calculations, the corresponding normalized correlation function should have noticeable oscillations even at values of l/Λ about 3–5. The normalized correlation function equals 2 in its principal maximum; additional peaks are lower. As the ratio l/Λ grows larger, the additional peaks become weaker, and at $l/\Lambda\gg 1$ both the intensity and the correlation function distributions have a one-peak shape with half width equal to Λ in the case of intensity and l in the case of the correlation function.

The experimental dependences presented in Figs. 2(a)–(c) correspond to l/Λ equal to 1, 1.3, and 1.7, respectively. For comparison, corresponding theoretical dependences calculated according to Eq. (5) are plotted in the same figure as solid curves. We had to take into account the noise (parasite Poissonian light). The signal-to-noise ratio, according to our measurements, was of order 100 in the maximum, and therefore the noise did not influence the intensity distribution. However, this noise turned out to be important for the correlation function distribution. It leads to the fast decay of correlation at large values of phase mismatch. The asymmetric shape of the correlation function distribution can be explained by a small phase mismatch in channel 1. (The corresponding fiber displacement is measured from the position of the correlation function central maximum; for all three spectra it was between 0.5 and 1 mm.) Also, the theoretical curves take into account the finite size of the measurement apertures (0.4 mm).

Thus, the oscillating character of the correlation function manifests itself under conditions when the intensity distribution shows no interference effects. It follows that measurement of the intensity correlation function together with the intensity distribution provides information about both the coherent length of the scattering excitations and the size of the scattering volume. To illustrate this, we measured the coordinates of the minima at the left-hand side of all three $g^{(2)}$ distributions from Fig. 2. (The right-hand-side minima are too few to make any conclusions.) According to the calculations, the distances between the minima should be inversely proportional to the beam diameter l: $x_n-x_{n+1}=\pi/l$. Calculating the values of l from the average distances between the minima in Figs. 2(a)–(c) we obtain 1.43±0.08, 2.1±0.1, and 2.4±0.2, respectively. Thus, the angular distribution of the correlation function indeed provides information about the scattering volume.

In our experiment, we used externally induced acoustic waves with quasithermal statistics. The same consideration can be given to any phase-matched scattering by equilibrium excitations. Certainly, in this case measurements of the intensity correlation function would require fast (picosecond) electronics. However, we hope that future experimental studies would allow this technique to be applied to the investigation of equilibrium excitations in spatially limited media. The observed oscillations have much in common with the speckles in the mean-square intensity distribution for light emitted by an incoherent source, calculated in Ref. [7]. Finally, it should be stressed that the fourth-order interference structure observed in the present paper has a purely classical nature. Fourth-order interference of fields with nonclassical correlation would provide a larger visibility [8,9].

We are indebted to D. N. Klyshko for valuable discussions. This work was supported in part by the Russian Foundation for Fundamental Investigations, Grant No. 96-02-16334a.

[1] R. H. Brown and R. Q. Twiss, Nature (London) **177**, 27 (1956).
[2] R. Q. Twiss, Opt. Act. **16**, 423 (1969).
[3] A. B. Haner and N. R. Isenor, Am. J. Phys. **38**, 6 (1970).
[4] S. P. Kulik, A. N. Penin, P. V. Prudkovsky, and M. V. Chekhova, Sov. Phys. JETP **110,** 11 (1996).
[5] D. N. Klyshko, *Photons and Nonlinear Optics* (Gordon and Breach, New York, 1987).
[6] M. Born and E. Wolf, *Principles of Optics* (Pergamon, New York, 1975).
[7] H. T. Yura, S. G. Hanson, and T. P. Grum, J. Opt. Soc. Am. A **10**, 316 (1993).
[8] J. G. Rarity *et al.*, Phys. Rev. Lett. **65**, 1348 (1990).
[9] D. N. Klyshko, Phys. Lett. A **163**, 349 (1992).